J. Chem. Eng. Data **2001,** *46,* 1025−1030

PρTx Measurements for Gas-Phase Pentafluoroethane + Propane Mixtures by the Burnett Method[†]

Yohei Kayukawa* and Koichi Watanabe

Department of System Design Engineering, Faculty of Science and Technology, Keio University,
3-14-1, Kohoku-ku, Yokohama 223-8522, Japan

In some refrigeration-based applications, hydrocarbons (HCs) are expected to be promising long-term alternative refrigerants because of their zero ozone depletion potential (ODP) and negligible global warming potential (GWP) values. But there exists a serious disadvantage that they are flammable. Despite their flammability, however, commercial demands for HCs are increasing not only in several European countries but also in southeast Asia. On the other hand, the flammability is considered a major issue in U.S.A. and Japan. To suppress the flammability, blended mixtures of HCs with nonflammable HFCs are considered. As one of such mixtures, pentafluoroethane (R-125) and propane (R-290) mixtures are dealt with in the present study. Although the thermodynamic properties of each single component have been studied rather extensively, there is no study reported on those of this binary system. Accordingly, we have measured the gas-phase *PρTx* properties of the binary R-125 (1) + R-290 (2) system by using the Burnett isothermal−isochoric coupling method. The present measurements cover an extensive range of temperatures (305 to 380 K), pressures up to 4.5 MPa, and densities up to 2.5 mol·dm^{-3} for the binary systems with four different mole fractions of x_1 = 0.00, 0.29, 0.50, and 0.75, respectively. The present paper discusses the gas-phase *PρTx* properties for the first time regarding the present binary mixtures at their selected compositions.

Introduction

In conjunction with an increasing concern about the global warming impact by the hydrofluorocarbon (HFC) refrigerants which have been proposed as being promising alternative refrigerants to replace several conventional chlorofluorocarbon (CFC) and/or hydrochlorofluorocarbon (HCFC) refrigerants, the refrigeration-based industries worldwide are facing another important issue to identify the long-term and environmentally benign alternatives.

Among the possible candidates along this line, there exists a possibility to blend the hydrocarbon (HC) refrigerants with some selected HFC compounds. Namely, an essential drawback of the flammability issue of HCs is expected to be reduced significantly by blending them with nonflammable HFCs, whereas the considerable global warming potential (GWP) of HFCs would be reduced by blending with HCs that have negligible GWP values. In the present study, therefore, we aimed to conduct a series of the gas-phase *PρTx* property measurements for the binary R-125 (1) + R-290 (2) mixture by the Burnett isothermal−isochoric coupling method. The present measurements cover an extended range of temperatures (305 to 380 K), and pressures up to 4.5 MPa, at four different compositions including pure R-290.

On the basis of the measurements, we have developed a simple truncated virial equation of state, and the thermodynamic behaviors with respect to the second and third virial coefficients, molar heat capacities, and speed of sound are also discussed in this paper.

Experimental Section

Figure 1 shows a schematic diagram of the experimental setup for the Burnett isothermal−isochoric coupling method. The apparatus consists of four subsystems: a cell system, a sample-filling system, a temperature control/measuring system, and a pressure control/measuring system.

The cell system consists of two cells, a sample cell (A) and an expansion vessel (B), and a constant-volume valve (V1) connecting the two cells. Both cells are thick walled spherical vessels made of SUS-304. The inner volume of the vessel is approximately 500 cm^3 for the sample cell, whereas it is 250 cm^3 for the expansion vessel. The cell constant, *N*, which is equivalent to the inner volume ratio of the two cells at zero pressure, is an essential factor to determine the density and the compressibility factor. It was precisely determined as N = 1.501 05 ± 0.000 10 by using gaseous helium, whose *PρT* properties are well-known.

A variable-volume vessel with metallic bellows (T) is a main part of the sample-filling subsystem. Since the sample composition is one of the important properties of the mixtures, we paid full attention to prepare the mixture sample as well as to charge it into the sample cell. Namely, the mixture sample with a known initial composition was prepared in a supplying vessel in advance and then transferred to the sample-charging variable-volume vessel

---

[†] This contribution will be part of a special print edition containing papers presented at the Fourteenth Symposium on Thermophysical Properties, Boulder, CO, June 25−30, 2000.

* To whom correspondence should be addressed.

10.1021/je000256k CCC: $20.00

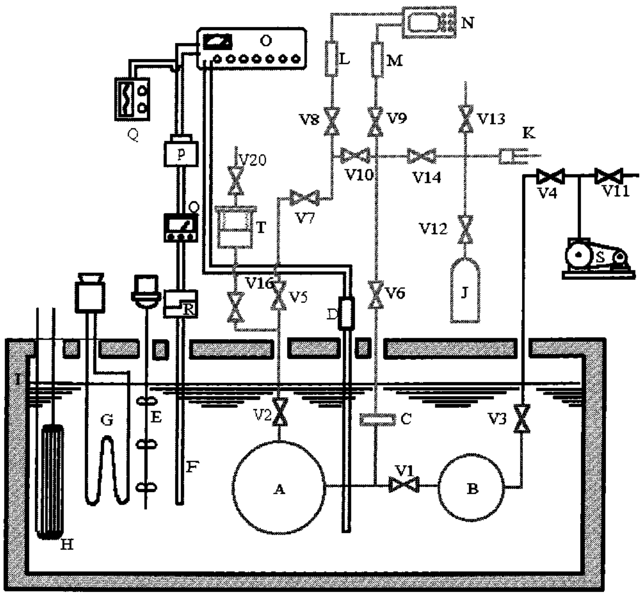

Figure 1. Schematic diagram of the experimental Burnett apparatus: (A) sample cell; (B) expansion cell; (C) differential pressure transducer; (D) platinum resistance thermometer; (E) stirrer; (F) subheater; (G) main heater; (H) water cooler; (I) constant-temperature bath; (J) N_2 bottle; (K) hand piston; (L, M) quartz pressure transducer; (N) digital pressure indicator; (O) thermometer bridge; (P) voltage/current converter; (Q) PID controller; (R) DC power supply; (S) vacuum pump; (T) variable-volume vessel; (V1) constant volume valve; (V2−V13) valves.

(T) with the metallic bellows. By filling high-pressure nitrogen gas at about 3 MPa inside the bellows, the sample outside was maintained as a compressed-liquid phase. Then, the specified quantity of sample was introduced into the sample cell little by little by opening the valve (V2) simultaneously, so that no composition change could be observed before and after the filling.

Regarding the temperature measurements, we assumed that the sample temperature is equivalent to the thermostated bath-fluid (silicone oil) temperature, being in thermodynamic equilibrium within a fluctuation of ±3 mK. A main heater (G) was used to increase the temperature, whereas a subheater (F) was used for controlling the temperature at the prescribed level. The subheater was controlled by a PID controller (R) according to the temperature detected by a standard platinum resistance thermometer (D) installed in the vicinity of the sample cell.

After temperature stability was confirmed, the sample pressure was measured with a differential pressure transducer (C) and quartz pressure transducers (L & M) at this state. We have used nitrogen gas as a pressure-transferring medium in the differential pressure transducer. The pressure difference between the sample and nitrogen gas must be carefully calibrated in advance as a function of temperature.

Note that we have successfully used the present Burnett apparatus to measure the thermodynamic properties of various refrigerants and their mixtures up to the present. Some of the latest publications include those for the binary mixtures R-32 + R-125[1] and R-125 + R-143a[2] by Zhang et al. and the ternary mixture R-32 + R-125 + R-143a by Tada et al.[3] and Kayukawa et al.[4]

According to the ISO recommendation,[5] the experimental uncertainties were estimated in terms of the expanded uncertainty with the coverage factor, being $k = 2$. The estimated uncertainties are not greater than ±7 mK in temperature, ±0.8 kPa in pressure, ±0.1% in density, and ±0.1 mol % in composition, respectively. Regarding the sample preparation, each single-component sample was blended on a mass-basis. They have research grade purities, that is, 99.953 mass % for R-125 and 99.9 mol % for propane, respectively. These sample purities are those analyzed by the chemical manufacturers, and we did not add any further purification.

Experimental Results

A total of 187 $P\rho Tx$ measurements of the binary R-125 (1) + R-290 (2) mixtures in their gaseous phase have been obtained in a range of temperatures (305 to 380 K), and pressures up to 4.9 MPa, at four different compositions with the mole fraction of R-125, $x_1 = 0.00$, 0.288, 0.500, and 0.750. They consist of the measurements along 6 isochores for pure R-290, those along 9 isochores for the mixture with $x_1 = 0.288$, those along 10 isochores with $x_1 = 0.500$, and those along 10 isochores with $x_1 = 0.750$, respectively. They all are tabulated in Table 1, where the compressibility factor, Z, and the molar density, ρ, are given at respective temperatures and pressures for four different compositions. Figure 2 illustrates a data distribution of these present measurements on a pressure−temperature diagram where the vapor-pressure curve for each pure component calculated from REFPROP (ver. 6.01)[6] is also included.

Discussion

On the basis of the present measurements, a thermodynamic model which represents the gas-phase $P\rho Tx$ properties of the binary R-125 (1) + R-290 (2) system in its entire range of compositions was developed. The present model is expressed as a truncated virial equation of state, for the compressibility factor, Z, as given below, where ρ denotes the molar density.

$$Z = 1 + B_m\rho + C_m\rho^2 + D_m\rho^3 \qquad (1)$$

where B_m, C_m, and D_m denote the second, third, and fourth mixture virial coefficients and they are given by eqs 2−4.

$$B_m = \sum_i^2 \sum_j^2 x_i x_j B_{ij} \qquad (2)$$

$$C_m = \sum_i^2 \sum_j^2 \sum_k^2 x_i x_j x_k C_{ijk} \qquad (3)$$

$$D_m = \sum_i^2 \sum_j^2 \sum_k^2 \sum_l^2 x_i x_j x_k x_l C_{ijkl} \qquad (4)$$

These mixture virial coefficients are obtained by applying a mixing rule to the second, third, and fourth cross virial coefficients, B_{ij}, C_{ijk}, and D_{ijkl}. Note that if $i = j = k = l$, each cross virial coefficient corresponds the virial coefficient for the pure component. It is generally well recognized, however, that most of the experimental $P\rho Tx$ property data in the gas-phase ever reported for different binary systems do not have sufficient accuracy and hence one could not determine the mixture fourth virial

Table 1. Experimental $P\rho Tx$ Properties for the Binary R-125 (1) + R-290 (2) System

T/K	P/kPa	ρ/mol·dm^{-3}	Z	T/K	P/kPa	ρ/mol·dm^{-3}	Z	T/K	P/kPa	ρ/mol·dm^{-3}	Z
					$x_1 = 0.00$						
380.000	3814.9	1.929	0.6263	365.000	1491.7	0.5707	0.8611	335.000	1324.4	0.5715	0.8318
380.000	2980.5	1.285	0.7335	365.000	1044.2	0.3802	0.9057	335.000	939.0	0.3807	0.8860
380.000	2204.9	0.8560	0.8142	365.000	718.9	0.2533	0.9363	335.000	651.5	0.2537	0.9232
380.000	1573.1	0.5703	0.8724	350.000	2539.6	1.287	0.6789	320.000	1238.1	0.5719	0.8128
380.000	1095.7	0.3799	0.9133	350.000	1939.3	0.8572	0.7774	320.000	885.4	0.3810	0.8733
380.000	751.8	0.2531	0.9415	350.000	1408.8	0.5711	0.8477	320.000	617.4	0.2538	0.9147
365.000	3447.5	1.930	0.5892	350.000	991.8	0.3805	0.8967	305.000	830.5	0.3813	0.8579
365.000	2763.5	1.286	0.7084	350.000	685.3	0.2535	0.9303	305.000	582.6	0.2540	0.9044
365.000	2073.6	0.8566	0.7973	335.000	1803.3	0.8579	0.7538				
					$x_1 = 0.288$						
380.000	4397.6	2.137	0.6513	365.000	246.3	0.08299	0.9814	335.000	334.5	0.1248	0.9661
380.000	3377.8	1.424	0.7485	350.000	3557.8	2.140	0.5705	335.000	225.0	0.08311	0.9773
380.000	2474.6	0.9485	0.8236	350.000	2912.6	1.426	0.6925	320.000	2210.6	1.428	0.6153
380.000	1756.4	0.6319	0.8784	350.000	2171.8	0.9499	0.7851	320.000	1858.6	0.9513	0.7325
380.000	1221.5	0.4210	0.9171	350.000	1571.2	0.6329	0.8523	320.000	1379.8	0.6338	0.8166
380.000	836.6	0.2805	0.9440	350.000	1104.2	0.4216	0.8995	320.000	984.4	0.4222	0.8755
380.000	567.9	0.1869	0.9623	350.000	761.5	0.2809	0.9321	320.000	685.3	0.2813	0.9160
380.000	382.8	0.1245	0.9747	350.000	518.9	0.1871	0.9544	320.000	469.5	0.1874	0.9436
380.000	257.1	0.08293	0.9831	350.000	350.6	0.1247	0.9694	320.000	318.3	0.1248	0.9622
365.000	3984.9	2.139	0.6139	350.000	237.1	0.08305	0.9795	320.000	214.3	0.08317	0.9747
365.000	3132.2	1.425	0.7226	335.000	3022.1	2.142	0.5195	305.000	1546.9	0.9520	0.6981
365.000	2322.8	0.9492	0.8058	335.000	2619.4	1.427	0.6573	305.000	1280.4	0.6342	0.7935
365.000	1664.4	0.6324	0.8663	335.000	2017.4	0.9506	0.7611	305.000	923.1	0.4225	0.8600
365.000	1163.1	0.4213	0.9090	335.000	1476.6	0.6333	0.8359	305.000	646.5	0.2815	0.9056
365.000	799.3	0.2807	0.9385	335.000	984.6	0.4219	0.8885	305.000	444.5	0.1875	0.9366
365.000	543.4	0.1870	0.9586	335.000	723.6	0.2811	0.9247	305.000	302.1	0.1249	0.9576
365.000	366.7	0.1246	0.9723	335.000	494.2	0.1873	0.9494	305.000	203.7	0.08323	0.9716
					$x_1 = 0.500$						
380.000	4917.4	2.454	0.6352	365.000	190.4	0.06350	0.9865	335.000	384.7	0.1433	0.9629
380.000	3779.6	1.635	0.7335	350.000	3926.7	2.458	0.5495	335.000	259.6	0.09545	0.9751
380.000	2785.8	1.089	0.8117	350.000	3194.1	1.637	0.6721	335.000	174.6	0.06359	0.9834
380.000	1988.1	0.7257	0.8697	350.000	2434.0	1.091	0.7688	320.000	2064.4	1.092	0.7106
380.000	1387.4	0.4835	0.9110	350.000	1772.1	0.7268	0.8401	320.000	1548.0	0.7278	0.8004
380.000	954.5	0.3221	0.9397	350.000	1252.8	0.4842	0.8909	320.000	1113.4	0.4849	0.8639
380.000	651.2	0.2146	0.9594	350.000	869.7	0.3226	0.9261	320.000	781.3	0.3230	0.9079
380.000	439.9	0.1430	0.9727	350.000	595.0	0.2149	0.9503	320.000	538.0	0.2152	0.9380
380.000	295.7	0.09524	0.9818	350.000	403.1	0.1432	0.9666	320.000	366.0	0.1434	0.9584
380.000	198.6	0.06345	0.9878	350.000	271.7	0.09538	0.9777	320.000	247.4	0.09551	0.9722
365.000	4429.2	2.456	0.5954	350.000	182.6	0.06354	0.9851	320.000	166.5	0.06363	0.9814
365.000	3490.4	1.636	0.7050	335.000	3400.6	2.460	0.4955	305.000	1431.7	0.7283	0.7747
365.000	2611.5	1.090	0.7917	335.000	2887.5	1.639	0.6338	305.000	1041.7	0.4852	0.8466
365.000	1880.9	0.7262	0.8559	335.000	2252.0	1.092	0.7421	305.000	736.5	0.3232	0.8963
365.000	1320.5	0.4838	0.9016	335.000	1661.4	0.7273	0.8219	305.000	509.1	0.2153	0.9303
365.000	911.9	0.3223	0.9334	335.000	1183.7	0.4845	0.8785	305.000	347.4	0.1435	0.9533
365.000	623.2	0.2147	0.9551	335.000	825.7	0.3228	0.9177	305.000	235.1	0.09558	0.9687
365.000	421.3	0.1431	0.9699	335.000	566.7	0.2150	0.9446	305.000	158.5	0.06368	0.9791
365.000	283.7	0.09531	0.9798								
					$x_1 = 0.750$						
380.000	4672.6	2.225	0.6645	365.000	170.8	0.05714	0.9880	335.000	346.8	0.1289	0.9665
380.000	3536.5	1.471	0.7583	350.000	3788.1	2.228	0.5851	335.000	233.9	0.08590	0.9776
380.000	2577.8	0.9803	0.8303	350.000	3013.2	1.474	0.7013	335.000	156.6	0.05723	0.9850
380.000	1825.8	0.6531	0.8831	350.000	2262.3	0.9818	0.7903	320.000	1931.4	0.9832	0.7365
380.000	1267.2	0.4351	0.9204	350.000	1631.5	0.6541	0.8556	320.000	1430.4	0.6550	0.8186
380.000	866.4	0.2899	0.9462	350.000	1145.1	0.4357	0.9016	320.000	1019.7	0.4364	0.8766
380.000	587.4	0.1931	0.9638	350.000	788.7	0.2903	0.9335	320.000	709.6	0.2907	0.9166
380.000	396.2	0.1287	0.9757	350.000	537.1	0.1934	0.9553	320.000	486.2	0.1937	0.9440
380.000	266.2	0.08571	0.9838	350.000	363.3	0.1288	0.9700	320.000	330.2	0.1290	0.9624
380.000	177.8	0.05710	0.9892	350.000	244.7	0.08584	0.9800	320.000	223.0	0.08596	0.9749
365.000	4236.6	2.227	0.6276	350.000	163.7	0.05719	0.9866	320.000	149.6	0.05727	0.9832
365.000	3278.2	1.473	0.7318	335.000	3320.6	2.230	0.5354	305.000	1755.4	0.9838	0.7016
365.000	2421.5	0.9810	0.8117	335.000	2739.7	1.475	0.6658	305.000	1325.8	0.6554	0.7950
365.000	1729.2	0.6536	0.8703	335.000	2099.4	0.9825	0.7656	305.000	955.5	0.4367	0.8607
365.000	1206.5	0.4354	0.9117	335.000	1532.1	0.6545	0.8386	305.000	669.2	0.2909	0.9059
365.000	828.2	0.2901	0.9403	335.000	1082.9	0.4361	0.8901	305.000	460.3	0.1938	0.9368
365.000	562.4	0.1933	0.9598	335.000	749.2	0.2905	0.9257	305.000	313.4	0.1291	0.9576
365.000	379.7	0.1288	0.9731	335.000	511.7	0.1935	0.9501	305.000	211.8	0.08602	0.9717
365.000	255.4	0.08578	0.9820								

coefficient, D_m, as accurately as possible to be represented by eq 4. We have applied, therefore, a simplified expression, eq 5, to substitute eq 4, since the present model is the simple truncated virial formulation without taking into account the fourth and higher virial terms.

$$D_m = \sum_i^2 x_i D_i \tag{5}$$

Both B_{ij} and C_{ijk} are expressed as functions of the reduced temperature, $T_r = T/T^*$, given in eqs 6 and 7,

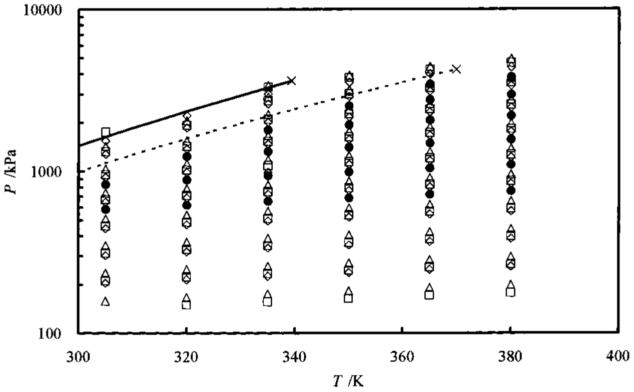

Figure 2. Experimental data distribution of R-125 (1) + R-290 (2): ●, $x_1 = 0.000$; ◇, $x_1 = 0.288$; △, $x_1 = 0.500$; □, $x_1 = 0.750$; —, vapor pressure curve for R-125; - - -, vapor pressure curve for R-290; ×, critical point.

respectively.

$$B_{ij} = b_{1,ij} + b_{2,ij}T_r^{-1} + b_{3,ij}\exp(T_r^{-1}) \tag{6}$$

$$C_{ijk} = c_{1,ijk} + c_{2,ijk}T_r^{-k_{1,ijk}} + c_{3,ijk}T_r^{-k_{2,ijk}} \tag{7}$$

D_i in eq 5 represents the pseudo-fourth virial coefficient to cover the remaining higher virial coefficients beyond the fourth one, and we have assigned a simple cubic function of reduced temperature as given in eq 8.

$$D_i = d_iT_r^{-3} \tag{8}$$

It should also be noted that the characteristic temperature, T^*, which is equivalent to the critical temperature, $T_{C,i}$, for the pure component, is defined in eqs 9 and 10 for the cross second and third virial coefficients, respectively, by employing the critical temperature values 339.165 K[8] for $T_{C,1}$ and 369.825 K[9] for $T_{C,2}$.

$$T^* = \sqrt{T_{C,i}T_{C,j}} \tag{9}$$

$$T^* = \sqrt[3]{T_{C,i}T_{C,j}T_{C,k}} \tag{10}$$

The functional form of eq 6 for the second virial coefficient was originally formulated by Zhang et al.[7] of our group for several HFC mixtures, whereas we have applied a conventional form for the third virial coefficient as given in eq 7.

B_{11}, C_{111}, and D_1 represent the contribution of the pure component R-125, and these numerical constants were obtained by the present authors[10] on the basis of their analysis of the Burnett measurements of Ye et al.[11] We have simply employed these numerical constants in the present modeling. On the other hand, the numerical constants which appear in eqs 6−8 for B_{22}, C_{222}, and D_2, which represent R-290, have been optimized and determined by means of our own least-squares fitting to the present measurements for R-290. The effectiveness of the representations for R-290 will be discussed later. We then obtained the numerical constants for the cross virial coefficients, B_{12}, C_{112}, and C_{122}, by means of the same optimum fitting procedure of eq 1 to the present measurements for the R-125 (1) + R-290 (2) mixture, at three different compositions. All of these numerical constants thus determined in the present study are tabulated in Table 2.

Table 2. Numerical Constants in Eqs 6−8

ij	$10b_{1,ij}$/dm^3·mol^{-1}	$10b_{2,ij}$/dm^3·mol^{-1}	$10b_{3,ij}$/dm^3·mol^{-1}
11	4.229 178	1.170 954	−2.979 276
22	2.622 157	4.636 876	−3.593 101
12	3.056 212	1.608 321	−2.454 742

ijk	$c_{1,ijk}$^{a}	$10^2c_{2,ijk}$^{a}	$10^3c_{3,ijk}$^{a}	$k_{1,ijk}$	$k_{2,ijk}$
111	$8.218\ 857 \times 10^{-4}$	2.697 741	−1.737 623	3	13
222	$2.101\ 379 \times 10^{-2}$	1.115 478	−6.818 215	7.5	9
112	-6.340769×10^{-3}	2.990 564	−2.165 380	3	11
122	$1.364\ 305 \times 10^{-2}$	1.592 396	−6.304 159	6	9

i	d_i/dm^9·mol^{-3}
1	$-2.287\ 655 \times 10^{-4}$
2	$-1.202\ 654 \times 10^{-3}$

[a] dm^6·mol^{-2}.

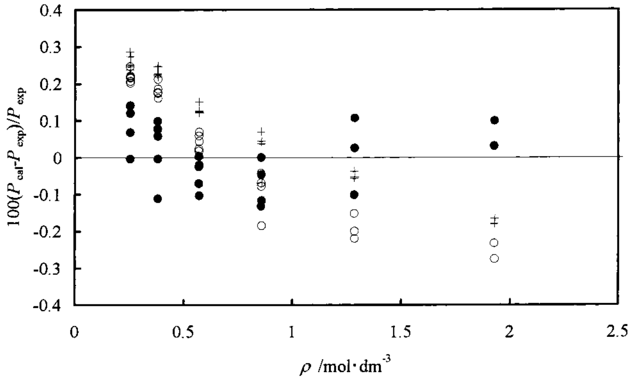

Figure 3. Relative pressure deviations calculated by different models from the present experimental data for pure R-290: ●, present model; ○, REFPROP (ver. 6.01);[6] +, Miyamoto and Watanabe.[12]

Figure 3 shows the relative pressure deviation, from the present measured results for R-290. For the purpose of simplicity to compare the present experimental data with available models including the present equation of state, eq 1, the dimensionless Helmholtz-function model recently proposed by Miyamoto and Watanabe,[12] and the prediction by REFPROP (ver. 6.01)[6] for pure R-290, the baseline in Figure 3 corresponds to the present data, while the ordinate values denote the pressure deviations of the calculated pressure values by different models mentioned above. It is obvious that the present model represents the measured $P\rho Tx$ properties with excellent reproducibility within ±0.13% in pressure. The present experimental $P\rho Tx$ properties deviate from those calculated from REFPROP by −0.28% to +0.25% in pressure, whereas those of the Miyamoto and Watanabe model from the present data are from −0.18% up to +0.28%. This fact confirms a satisfactory reliability of the present measurements as well as the present thermodynamic model for pure R-290. The temperature dependence of the second virial coefficient for R-290 will be discussed later, together with those for the binary R-125 (1) + R-290 (2) mixture.

Figure 4 illustrates a similar comparison in terms of the relative pressure deviation of the calculated pressure values by the present model and the prediction of REFPROP from the present data for the binary R-125 (1) + R-290 (2) mixture. It is apparent that the present model provides excellent reproducibility of the present experimental data with $x_1 = 0.500$ and 0.750 within ±0.39% in pressure, while its representation of the lower density data for the mixture with x_1 = 0.288 deviates by +0.69% maximum. The predicted values from REFPROP deviate more than those

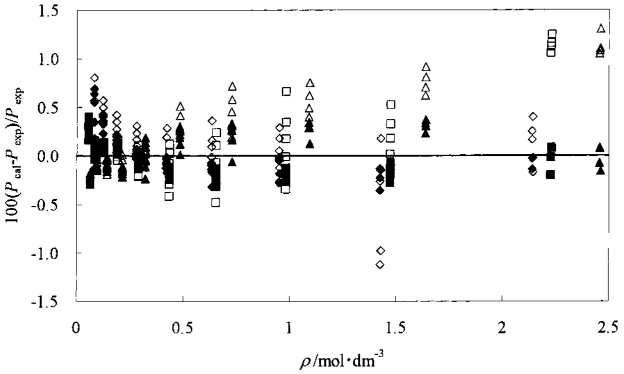

Figure 4. Relative pressure deviations calculated by different models from the present experimental data for the binary R-125 (1) + R-290 (2): ◆, this work, $x_1 = 0.288$; ▲, this work, $x_1 = 0.500$; ■, this work, $x_1 = 0.750$; ◇, REFPROP (ver. 6.01),[6] $x_1 = 0.288$; △, REFPROP, $x_1 = 0.500$; □, REFPROP, $x_1 = 0.750$.

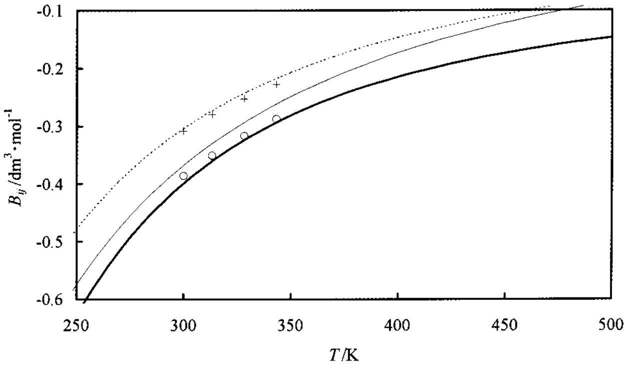

Figure 5. Temperature dependence of the second virial coefficients of the present model: —, B_{11} this work; **—**, B_{22} this work; - - -, B_{12} this work; +, B_{12}, McElroy;[13] ○, B_{22}, McElroy.[13]

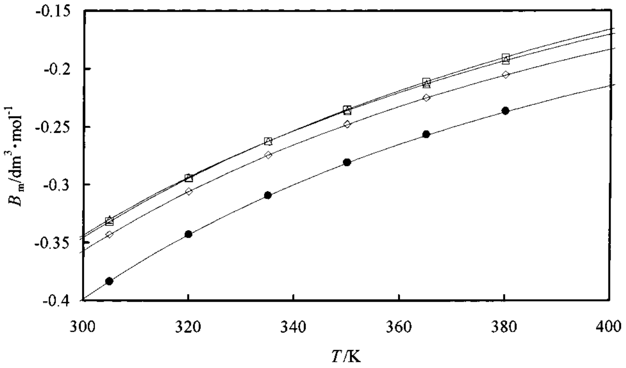

Figure 6. Temperature dependence of the experimental second virial coefficients for the R-125 (1) + R-290 (2) system, B_m: ●, $x_1 = 0.000$, i.e., B_{22}; ◇, $x_1 = 0.288$; △, $x_1 = 0.500$; □, $x_1 = 0.750$; —, calculated curves by the present model.

of our model, almost to ±1% in pressure with the deviations becoming more significant at higher densities.

Figure 5 shows the temperature dependence of the calculated second virial coefficients, B_{11} and B_{22}, and the cross virial coefficient, B_{12}. The caluculated B_{22} and B_{12} values reported by McElroy[13] are also included in this figure. It is found that the second virial coefficients exhibit thermodynamically sound behavior with temperature. The cross virial coefficient, B_{12}, has a larger value than those of both R-125 and R-290, and this fact suggests that the present binary system exhibits a strong positive pressure azeotrope. The B_{22} and B_{12} values of McElroy agree well with those calculated from the present model within ±3.3% for B_{22} and ±3.7% for B_{12}, respectively. Our experimental values of the mixture second virial coefficient, B_m, that were determined by extrapolating the $(Z - 1)/\rho$ values to the zero density, are shown at different temperatures in Figure 6 together with the curves calculated from the conventional mixing rules given in eq 2. The present experimental values are well represented by the present model. The relative deviations of these experimental second virial coefficient values from our model are illustrated in Figure 7, and it is apparent that the experimental second virial coefficients are well represented within ±0.4%. The reproducibility of the present model for the mixtures is better than that for pure R-290, since we could not find enough isothermal data for R-290 to determine precisely the experimental second virial coefficient.

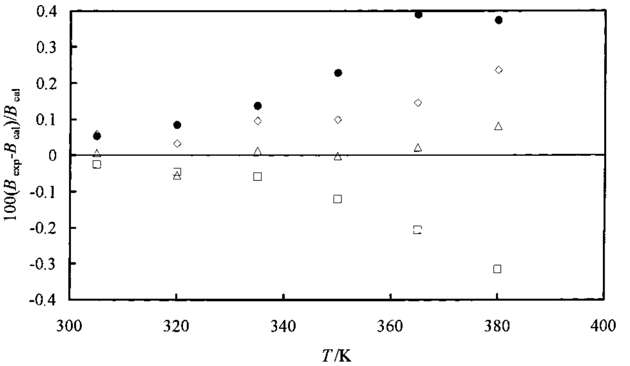

Figure 7. Relative deviations of the experimental second virial coefficients, B_m, from the present model: ●, $x_1 = 0.000$, i.e., B_{22}; ◇, $x_1 = 0.288$; △, $x_1 = 0.500$; □, $x_1 = 0.750$.

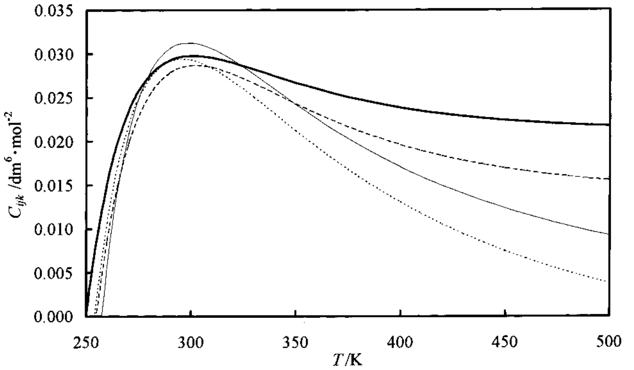

Figure 8. Temperature dependence of the third virial coefficients of the present model: —, C_{111} this work; **—**, C_{222} this work; · · ·, C_{112} this work; - - -, C_{122} this work.

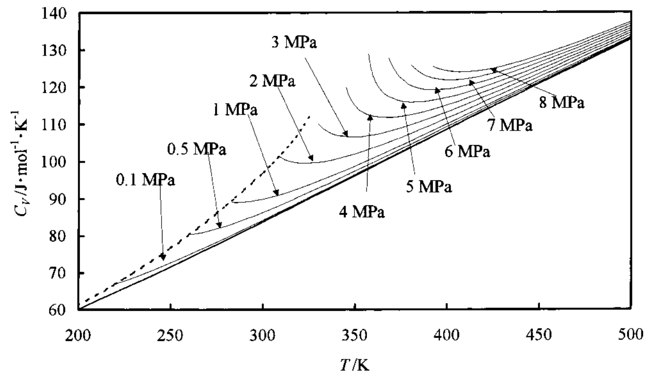

Figure 9. Temperature dependence of isochoric heat capacity for the binary 0.500 R-125 (1) + 0.500 R-290 (2) with the mole fraction of R-125, $x_1 = 0.500$; —, isobars for 0.1, 0.5, 1, 2, 3, 4, 5, 6, 7, and 8 MPa; **—**, ideal gas; - - -, saturation.

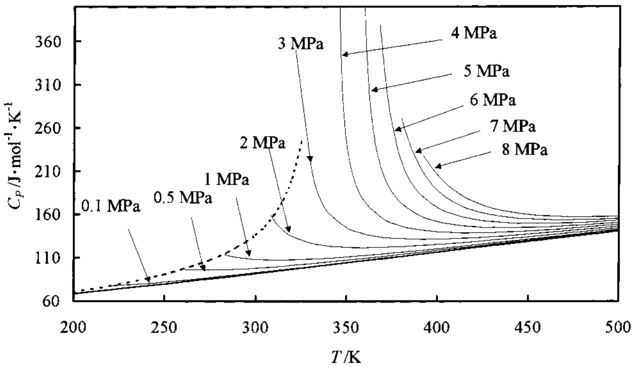

Figure 10. Temperature dependence of isobaric heat capacity for the binary 0.500 R-125 (1) + 0.500 R-290 (2) with the mole fraction of R-125, x_1 = 0.500; —, isobars for 0.1, 0.5, 1, 2, 3, 4, 5, 6, 7, and 8 MPa; **—**, ideal gas; - - -, saturation.

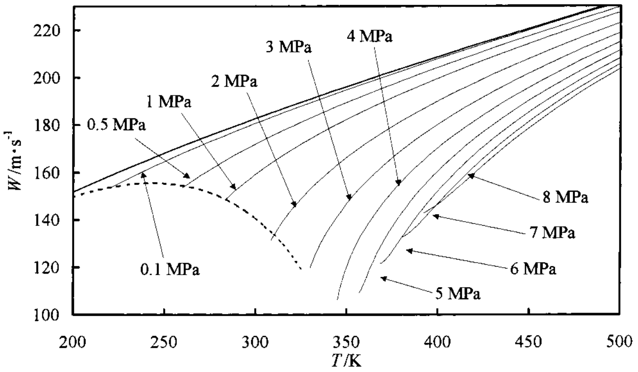

Figure 11. Temperature dependence of speed of sound for the binary 0.500 R-125 (1) + 0.500 R-290 (2) with the mole fraction of R-125, x_1 = 0.500; —, isobars for 0.1, 0.5, 1, 2, 3, 4, 5, 6, 7, and 8 MPa; **—**, ideal gas; - - -, saturation.

The reproducibility of the mixture third virial coefficients by the present model is not discussed in this paper, since the present measurements do not have enough accuracy to obtain reliable experimental third virial coefficient values. However, we have confirmed thermodynamically sound behavior of the temperature dependence of the excess third virial coefficient predicted from the present model shown in Figure 8, and this should have definitive effects on the derived property behaviors. In the present discussion, derived properties such as molar isochoric heat capacity, molar isobaric heat capacity, and speed of sound are also examined. These properties are derived from the present model and the ideal gas heat capacities calculated from the ideal gas heat capacity correlation for R-125 by Ogawa et al.[14] and the ideal part of the Helmholtz-function model for R-290 by Miyamoto and Watanabe.[12]

Temperature dependences of derived properties thus calculated by the present model are illustrated in Figures 9−11. It is readily found that these derived properties provide thermodynamically sound behavior not only in the present measured temperature and pressure range but also in the extensive range of temperatures (200 to 500 K) and pressures up to 8 MPa. In the supercritical region, the present model still exhibits the rational behavior of those derived properties around the vicinity of the critical density, 5 mol·dm^{-3}.

Conclusions

A total of 187 gas-phase $P\rho Tx$ measurements for the binary R-125 (1) + R-290 (2) system have been reported over an extensive range of temperatures and pressures at four different compositions. This is the first set of data ever reported for the gas-phase $P\rho Tx$ properties of this binary refrigerant system. On the basis of the present measurements, a thermodynamic model was developed. The model represents our experimental $P\rho Tx$ properties and the virial coefficients for the present binary system including pure components with sufficient accuracy. The developed model has been confirmed to provide a thermodynamically consistent representation of the $P\rho Tx$ properties and the derived properties for this binary system of present interest.

Literature Cited

(1) Zhang, H.-L.; Sato, H.; Watanabe, K. Gas Phase *PVT* Properties for the Difluoroethane + Pentafluoroethane (R-32 + 125) System. *J. Chem. Eng. Data* **1996**, *41*, 1401−1406.

(2) Zhang, H.-L.; Sato, H.; Watanabe, K. *PVTx* Properties in the Gas Phase for Binary R-125/143a System. *Fluid Phase Equilib.* **1998**, *150*, 333−341.

(3) Tada, S.; Zhang, H.-L.; Sato, H.; Watanabe, K. Mesurements of Gas-phase *PVTx* Properties of the Ternary R-32/125/143a Mixture. *Proceedings of the 5th Asian Thermophysical Properties Conference*, Seoul, Korea, 1998; pp 269−272.

(4) Kayukawa, Y.; Tada, S.; Zhang, H.-L.; Watanabe, K. Mesurements of Gas-phase *PVTx* Properties for the Ternary R-32/125/143a Mixture. *Proceedings of the 20th International Congress of Refrigeration* (CD-ROM), Sydney, Australia, 1999; Vol. II, Paper 395, pp 2049−2056.

(5) *International Organization of Standardization. Guide to the Expression of Uncertainty in Measurement*; ISO: Switzerland, 1993.

(6) McLinden, M. O.; Kein, S. A.; Lemmon, E. W.; Peskin, A. P. REFPROP, Thermodynamic and Transport Properties of Refrigerants and Refrigerant Mixtures. Standard Reference Database 23−Version 6.01; NIST: U.S. Secretary of Commerce on behalf of the United States of America, 1998.

(7) Zhang, H.-L.; Sato, H.; Watanabe, K. Second Virial Coefficients for R-32, R-125, R-143a, R-152a and Their Binary Mixtures. *Proceedings of the 19th International Congress of Refrigeration*, The Hague, The Netherlands, 1995; Vol. IVa, pp 622−629.

(8) Kuwabara, S.; Aoyama, H.; Sato, H.; Watanabe, K. Vapor-Liquid Coexistence Curve in the Critical Region and the Critical Temperatures and Densities of Difluoroethane and Pentafluoroethane. *J. Chem. Eng. Data* **1995**, *40*, 112−116.

(9) Thomas, R. H. P.; Harrison, R. H. Pressure−Volume−Temperature Relations of Propane. *J. Chem. Eng. Data* **1982**, *27*, 1−11.

(10) Kayukawa, Y.; Watanabe, K. Thermodynamic Modeling of the Gas-Phase *PVTx* Properties for the Ternay R-32/125/143a System. Paper presented at *14th Symposium on Thermophysical Properties*, Boulder, CO, 2000; submitted to *Int. J. Thermophys.* for reviewing.

(11) Ye, F.; Sato, H.; Watanabe, K. Gas-phase *PVT* Properties and Vapor Pressures of Pentafluoroethane (HFC-125) Determined According to the Burnett Methodology. *J. Chem. Eng. Data* **1995**, *40*, 1, 148−152.

(12) Miyamoto, H.; Watanabe, K. A Thermodynamic Model for Fluid-Phase Propane. *Int. J. Thermophys.* **2000**, *21*, *5*, 1045−1072.

(13) McElroy, P. J. Excess and Unlike-Interaction 2nd Virial-Coefficients and Excess Molar Enthalpy of a Refrigerant Mixture (0.500CH_2FCF_3 + 0.500C_3H_8). *J. Chem. Thermodyn.* **1995**, *27*, 1047−1052.

(14) Ogawa, K.; Kojima, T.; Sato, H. Paper presented at *14th Symposium on Thermophysical Properties*, Boulder, CO, 2000.

Received for review August 4, 2000. Accepted December 11, 2000.

JE000256K